International Journal of Fracture 38: 143–155 (1988)

The stress field in an edge cracked plate in anti-plane deformation

V.C. LI and H. S. LIM

Department of Civil Engineering, Massachusetts Institute of Technology, Cambridge, MA 02139, USA

Received 21 August 1987; accepted in revised form 24 March 1988

Abstract. The anti-plane strain problems of an edge cracked elastic plate under 1) uniform surface displacement load and 2) surface line loads are solved using conformal mapping techniques. The solutions yield stress, strain and displacement distributions and stress intensity factors in the plate.

The line load solutions can be used as Green's functions to obtain further solutions for more general surface loading conditions. As an application, we calculate the strain field on the upper plate surface due to arbitrarily imposed tractions on the lower plate surface, using a superposition technique and the Green's functions just mentioned.

In addition, the stress intensity factors for two edge cracks with arbitrary length ratios and distance of separation have been worked out.

1. Introduction

A number of anti-plane crack problems have been solved (see, e.g., Tada et al. [1]; Paris and Sih [2]; Tse et al. [3]). This paper presents the full elastic solution for two edge crack problems using analytic function theory and conformal mapping techniques. The edge cracked elastic plate is subjected to surface loading, with the plate of thickness H and edge crack length "a", and loading configurations as shown in Figs. 1 and 2. In the first case (Fig. 1) the loading is imposed by uniform (with opposite signs on either side of the crack) displacement. Multiple conformal mappings transform this geometry into a rectangle with two edges loaded by equal and opposite displacements, and the remaining edges of the rectangle are traction free. In the second case (Fig. 2) the loading is imposed by two line loads (again with opposite signs on either side of the crack) at any arbitrary distance from the crack. Multiple conformal mappings transform this geometry into a half space with a traction free surface except for two equal and opposite line loads. For both problems, the elastic solution on the mapped planes are readily available. This method also generates the solution for the problem when the line loads are imposed directly on the crack faces.

The solution for the second case is particularly useful as it can be used as Green's functions to generalize the solution to that for any arbitrary distribution of surface tractions. As an example, we use this technique to calculate the surface strain due to distributions of basal tractions obtained from an analysis by Li and Rice [4] of an edge cracked elastic plate mechanically coupled to a viscoelastic foundation. In addition, the stress intensity factor for a pair of edge cracks can be worked out based on the full elastic solutions for the single edge crack problem, and is also presented in this paper.

The boundary value problems described above originated from analyses of surface deformations at transform tectonic plate margins, but the solutions could be useful for other applications such as analyzing structural plates with elongated surface flaws.

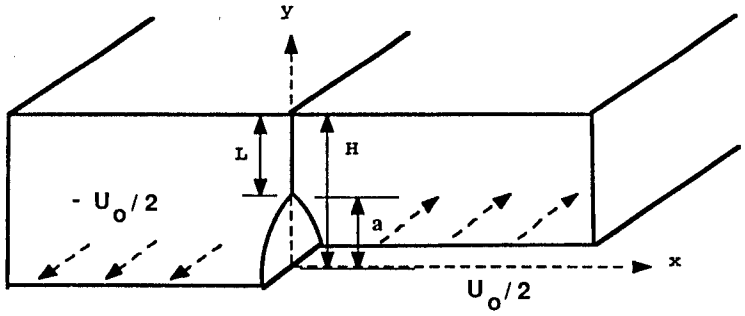

Fig. 1. Cross-sectional view of edge cracked plate loaded by uniform (with opposite signs on either side of crack) displacement.

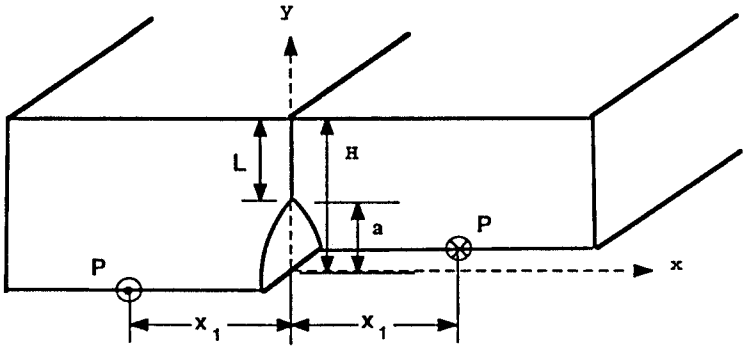

Fig. 2. Cross-sectional view of edge cracked plate loaded by line loads (with opposite signs on either side of crack) at distance x_1 from the crack.

2. Case with uniform imposed displacement

Elasticity theory leads to the governing equation for the only non-vanishing displacem $u(x, y)$:

$$\nabla^2 u = 0$$

subject to the "basal" loading

$$u(x, y = 0) = \begin{cases} u_0/2 & \text{for } x > 0 \\ -u_0/2 & \text{for } x < 0 \end{cases},$$

where u_0 is an imposed relative displacement. The displacement and shear stres can be represented in terms of an analytic function $\Phi(\mathbf{Z})$ of the complex variable $\mathbf{Z}$ $x + iy$:

$$u = C \operatorname{Re} [\Phi(\mathbf{Z})]$$

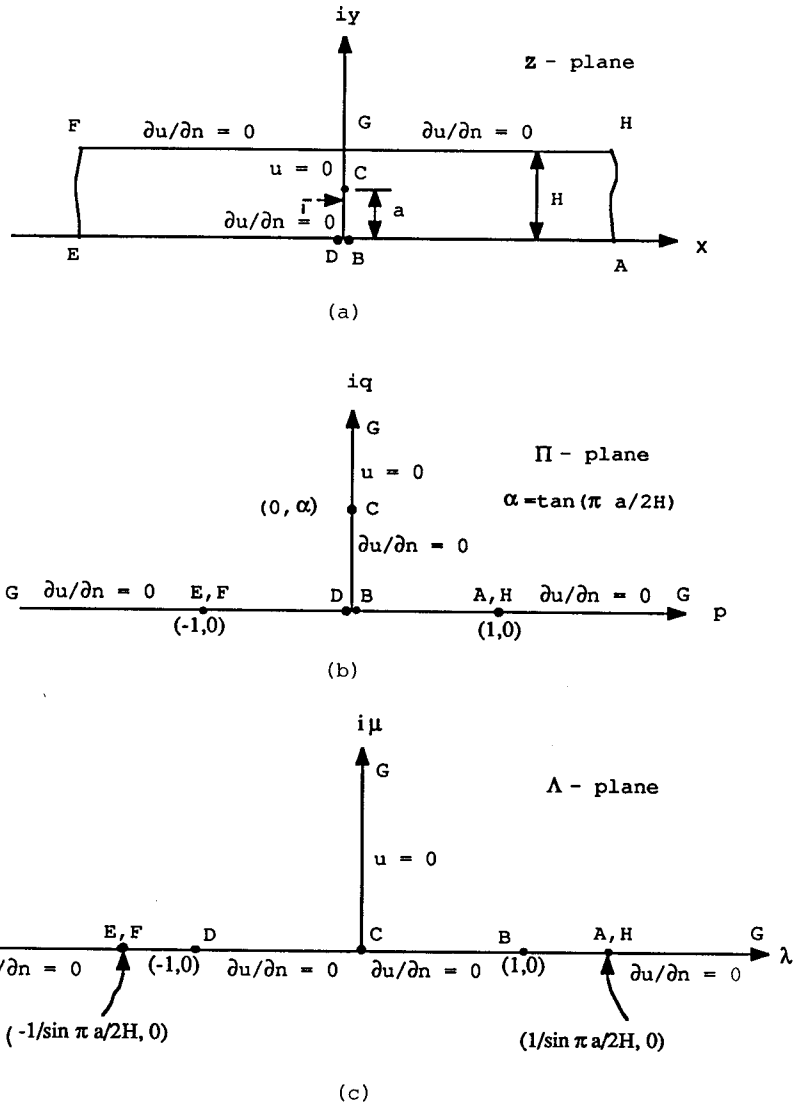

Fig. 3. Conformal mappings to transform the physical plane of an edge cracked infinitely long strip into a half-space.

and

$$\tau_{xz} - i\tau_{yz} = GC\Phi'(\mathbf{Z}), \tag{4}$$

where G is the shear modulus and C is a constant to be determined.

Our objective is to solve for Φ satisfying all the boundary conditions as shown in Fig. 3a and in (2), and using analytic function theory and standard conformal mapping techniques. (Capital lettering has been used in the figures to show the mapping of corresponding points on the physical and mapped planes). Figure 3b is a result of mapping the physical (infinitely long) rectangular $\mathbf{Z}$ plane into the (upper half of the) Π $(=p + iq)$ plane using

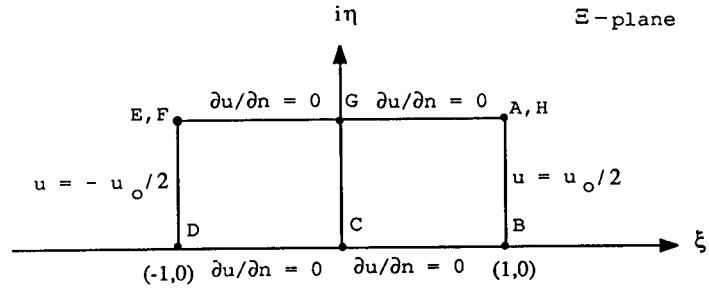

Fig. 4. Conformal mapping to transform the half-space into a finite rectangular box.

the mapping function

$$\Pi = \tanh(\pi \mathbf{Z}/2H). \tag{5}$$

In the Π-plane the crack DCB is still inside the upper half space. The next step is to fold this out to become part of the surface of the half space. This is achieved by the mapping function

$$\Lambda = \sqrt{1 + \Pi^2/\tan^2(\pi a/2H)}, \tag{6}$$

where $\Lambda = \lambda + i\mu$. In the Λ-plane (Fig. 3c) the imposed displacement boundary conditions at the base of the plate in the physical plane are now mapped into the same conditions on the two associated line segments ED and BH. To map the Λ-plane into a finite rectangular box (Fig. 4), a somewhat complicated mapping function is needed in the form of

$$\Xi = F(k_1, \sin^{-1}\Lambda)/F(k_1, \pi/2), \tag{7}$$

where $\Xi = \xi + i\eta$, $k_1 = \sin(\pi a/2H)$. The function F is the elliptic integral of the first kind defined by

$$F(k, \varphi) = \int_0^{\varphi} \frac{\mathrm{d}\varphi}{\sqrt{1 - k^2 \sin^2 \varphi}}. \tag{8}$$

In the Ξ plane the original physical domain is now mapped into a simple rectangle with height given by $F(k_1', \pi/2)/F(k_1, \pi/2)$, where $k_1' = \cos(\pi a/2H)$, and length given by 2. With the traction free boundary condition on two opposite horizontal sides, and the imposed displacement $u_0/2$ and $-u_0/2$ on the remaining opposite vertical sides (Fig. 4) the solution for the displacement u in the Ξ-plane is simply observed to be a linear function of ξ. Hence

$$u(\Xi) = (u_0/2)\xi. \tag{9}$$

Comparison of (9) with (3) reveals that the analytic function Φ is simply Ξ and the constant C is $u_0/2$. Using (3) and the mapping functions (5), (6) and (7), the displacement field in the

plate can be written as

$$u(\mathbf{Z}) = \frac{u_0}{2} \operatorname{Re} \frac{F(k_1, \sin^{-1}[\Omega(\mathbf{Z})])}{F(k_1, \pi/2)}, \tag{10}$$

where $\Omega(k) = \sqrt{[1 + \tanh^2(\pi k/2H)/\tan^2(\pi a/2H)]}$.

The shear stresses in the body can be obtained using (4) and the mapping functions (5), (6) and (7), and are given by

$$\tau_{xz} - \mathrm{i}\tau_{yz} = \frac{\mathrm{i}G(u_0/2)(\pi/2H)\operatorname{sech}(\pi\mathbf{Z}/2H)}{F(k_1, \pi/2)\sin(\pi a/2H)\Omega(\mathbf{z})} \tag{11}$$

and the surface strain at $y = H$ is then

$$\gamma_s(x) = \frac{(u_0/2)(\pi/2H)}{F(k_1, \pi/2)\sin(\pi a/2H)\sinh(\pi x/2H)\Omega(x + \mathrm{i}H)} \tag{12}$$

The mode III stress intensity factor can be derived using (11) and by making use of the form of the asymptotic crack tip field (e.g., Rice [5])

$$K_{\mathrm{III}} = \lim_{y \to a} \sqrt{2\pi(y - a)}\,\tau_{xz}. \tag{13}$$

Hence,

$$K_{\mathrm{III}} = \frac{G(u_0/2)(\pi/2H)\sqrt{2H}}{F(k_1, \pi/2)\sqrt{\sin(\pi a/2H)\cos(\pi a/2H)}}. \tag{14}$$

The above solutions can be shown (Lim [6]) to satisfy all the boundary conditions, as required.

3. Case with line loads

The mapping functions (5) and (6) can be used again to map the physical plane shown in Figs. 2 and 3a into the Π and Λ planes shown in Figs. 3b and 3c. For the present loading conditions, the line loads are mapped inside the line segments ED and BH, which lie on the otherwise traction free surface of the half space in the Λ-plane. The solution of line loads acting on the surface of elastic half space is well known (one analogy is the solution for the problem in hydrodynamics involving a source and a sink of equal strength placed at equal distances on opposite sides of the origin). For the two line loads of magnitude P (force per unit length) acting at $x = \pm x_1$ in the present problem, the displacement field can be directly wirtten in the Λ plane as

$$u(\Lambda) = -\frac{P}{\pi G} \operatorname{Re} \log \left[\frac{\Lambda - \Omega(x_1)}{\Lambda + \Omega(x_1)} \right]. \tag{15}$$

Comparison between (15) and (3) reveals that the analytic function Φ for this problem is

$$\Phi = \log\left[\frac{\Lambda - \Omega(x_1)}{\Lambda + \Omega(x_1)}\right] \tag{16}$$

and the constant C is $-P/(\pi G)$.

Using (3), (5), (6) and (16), the displacement field in the plate can be written as

$$u(\mathbf{Z}) = -\frac{P}{\pi G}\,\mathrm{Re}\log\left[\frac{\Omega(\mathbf{Z}) - \Omega(x_1)}{\Omega(\mathbf{Z}) + \Omega(x_1)}\right]. \tag{17}$$

The shear stresses in the body can be obtained from (4) and (16) and are given by

$$\tau_{xz} - \mathrm{i}\tau_{yz} = -\frac{P}{H}\frac{\Omega(x_1)\tanh(\pi\mathbf{Z}/2H)\,\mathrm{sech}^2(\pi\mathbf{Z}/2H)}{[\tanh^2(\pi\mathbf{Z}/2H) - \tanh^2(\pi x_1/2H)]\Omega(\mathbf{Z})} \tag{18}$$

Similarly the surface ($y = H$) strain field can be written as

$$\gamma_s(x) = \frac{P}{GH}\frac{\Omega(x_1)\tanh(\pi x/2H)\,\mathrm{csch}^2(\pi x/2H)}{[1 - \tanh^2(\pi x/2H)\tanh^2(\pi x_1/2H)]\Omega(x + \mathrm{i}H)}. \tag{19}$$

The mode III stress intensity factor can be derived using (13) and (18) from the stress distribution along the crack line ($x = 0$). It is given by

$$K_{\mathrm{III}} = \frac{P}{H}\frac{\sqrt{2H\tan(\pi a/2H)}}{\sin(\pi a/2H)\Omega(x_1)} \tag{20}$$

The stress intensity factor (20) is found to coincide with that given by Tada *et al.* [1] which was obtained using asymptotic interpolation method. The above solutions can be shown to satisfy all the boundary conditions (Lim [6]).

Note that the conformal mapping method used here is just as applicable for the problem when the crack faces are loaded by line forces. Indeed the mapping would be exactly the same, only that the line-forces are now applied in the line segment CD and CB instead of DE and BA. Since all these line segments are on the surface of the half-plane in the mapped Λ-plane, the solution procedure is identical to the one presented above. For crack face loading at $y = y_1$, the displacement field in the plate is

$$u(\mathbf{Z}) = -\frac{P}{\pi G}\,\mathrm{Re}\log\left[\frac{\Omega(\mathbf{Z}) - \Omega(\mathrm{i}y_1)}{\Omega(\mathbf{Z}) + \Omega(\mathrm{i}y_1)}\right] \tag{21}$$

and the shear stresses in the plate are given by

$$\tau_{xz} - \mathrm{i}\tau_{yz} = -\frac{P}{H}\frac{\Omega(\mathrm{i}y_1)\tanh(\pi\mathbf{Z}/2H)\,\mathrm{sech}^2(\pi\mathbf{Z}/2H)}{[\tanh^2(\pi\mathbf{Z}/2H) + \tan^2(\pi y_1/2H)]\Omega(\mathbf{Z})}. \tag{22}$$

The mode III stress intensity factor is

$$K_{III} = \frac{P\sqrt{2H \tan(\pi a/2H)}}{H \sin(\pi a/2H)\Omega(iy_1)}, \tag{23}$$

which coincides with that given by Tada et al. [1].

4. Application of line load solutions as Green's functions

The line load solutions given in (17) to (20) above can be used as Green's functions in order to extend the solution to cases where the plate basal tractions are arbitrarily distributed. The well known superposition method is applicable as the problem is linear, so that

$$Q(x) = \int_0^\infty G(x, x')\, dP(x'). \tag{24}$$

In the general formulation (23), $Q(x)$ can represent any of the deformation fields, $G(x, x')$ is the appropriate Green's function describing the quantity Q at x caused by a line load at x', and dP is the magnitude of the line load at x' given by $\tau(x')\, dx'$, where $\tau(x')$ is the basal traction at x'. As a specific application we use (19) as the Green's function to calculate the surface ($y = H$) strain due to distributions of basal traction (in the form of a shear stress rate) shown in Fig. 5. These traction rate distributions $\dot{\tau}(x)$ have been obtained from an analysis by Li and Rice [4] of an edge cracked elastic plate coupled to a viscoelastic foundation in connection with the analysis of surface deformation profiles at tectonic plate boundaries. Using (19) and (24) the surface strain rate can be calculated from

$$\dot{\gamma}_s(x) = \int_0^\infty \frac{\Omega(x_1) \tanh(\pi x/2H)\, \operatorname{csch}^2(\pi x/2H)\dot{\tau}(x_1)\, dx_1}{GH[1 - \tanh^2(\pi x/2H) \tanh^2(\pi x_1/2H)]\Omega(x + iH)} \tag{25}$$

as is shown in Fig. 6.

5. Double edge cracked elastic plate

The line load solutions for the case when the crack faces are loaded by line forces can be used in conjunction with an alternative superposition technique to solve for the problem of a double edge cracked plate under anti-plane loading. We demonstrate this procedure by calculating the stress intensity factor of an elastic plate of thickness H with two adjacent cracks of length "a" and "b" separated a distance "d" apart and is subjected to a remotely applied load as shown in Fig. 7.

The approach here is to first treat the problem as an elastic plate containing a single edge crack of length "a" loaded remotely by a load σ. The solution to this problem is well-known (see, e.g., Turcotte and Spence [7]). In order to simulate traction-free conditions along the crack faces of crack "b", tractions of equal magnitude and opposite signs will have to be applied at the location of the second crack. These applied tractions will in turn induce

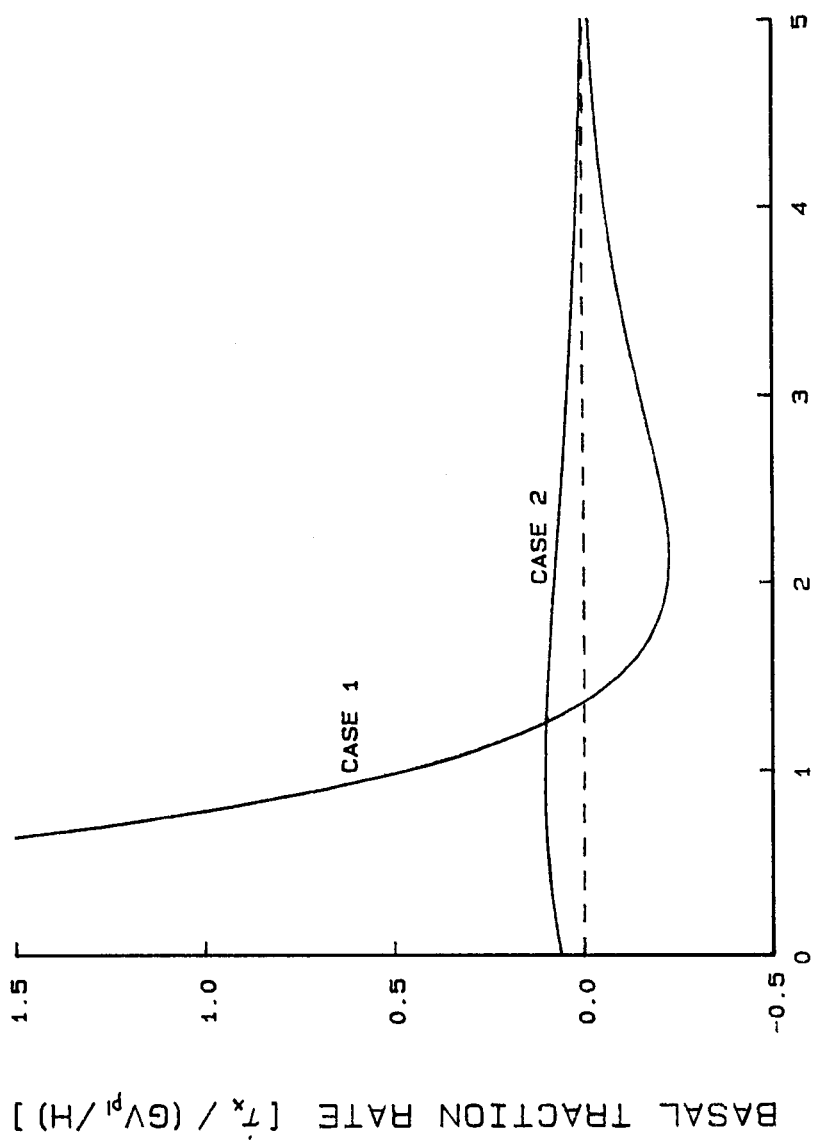

Fig. 5. Distributions of basal traction obtained from an analysis by Li and Rice [4] of an edge cracked elastic plate mechanically coupled to a viscoelastic foundation. Case 1 represents a very concentrated distribution of basal traction near the crack. Case 2 represents a broad distribution of basal tractions.

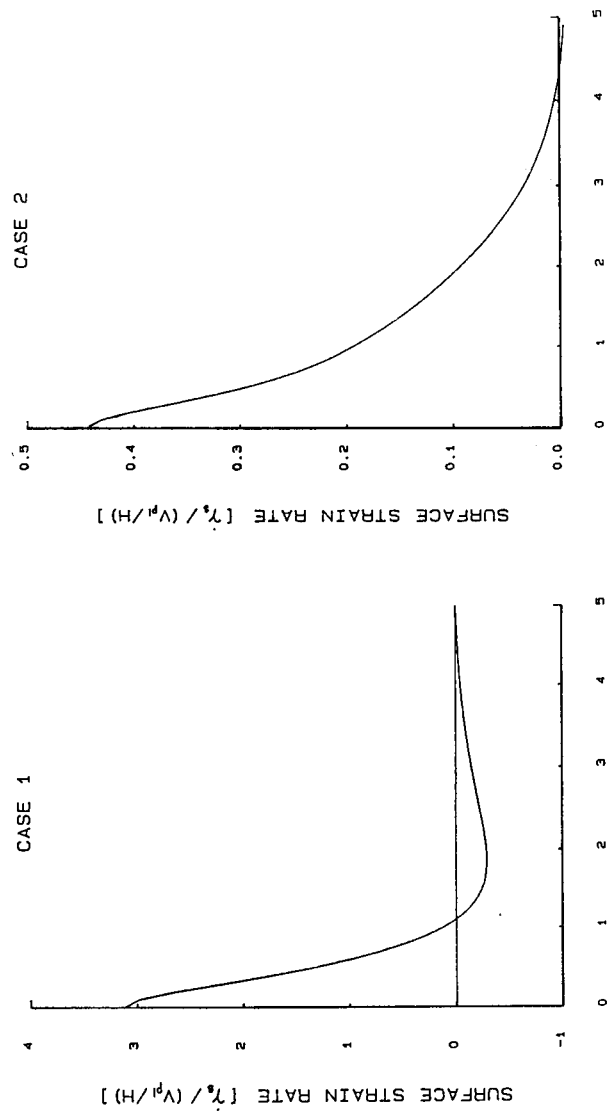

Fig. 6. Surface strain rate profile associated with the two distributions of basal traction shown in Fig. 5.

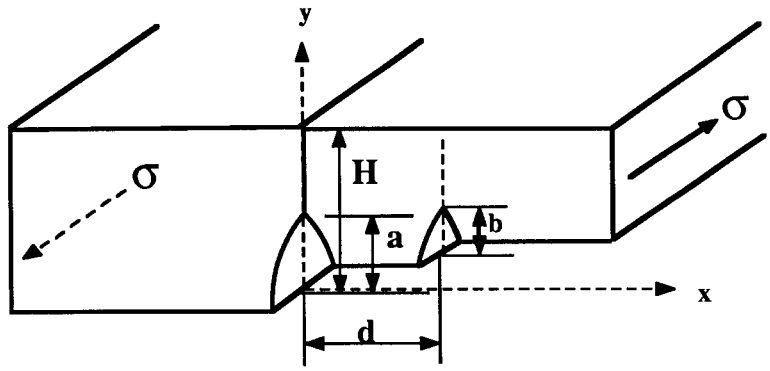

Fig. 7. Cross-sectional view of double edge cracked plate loaded by remotely applied line force σ.

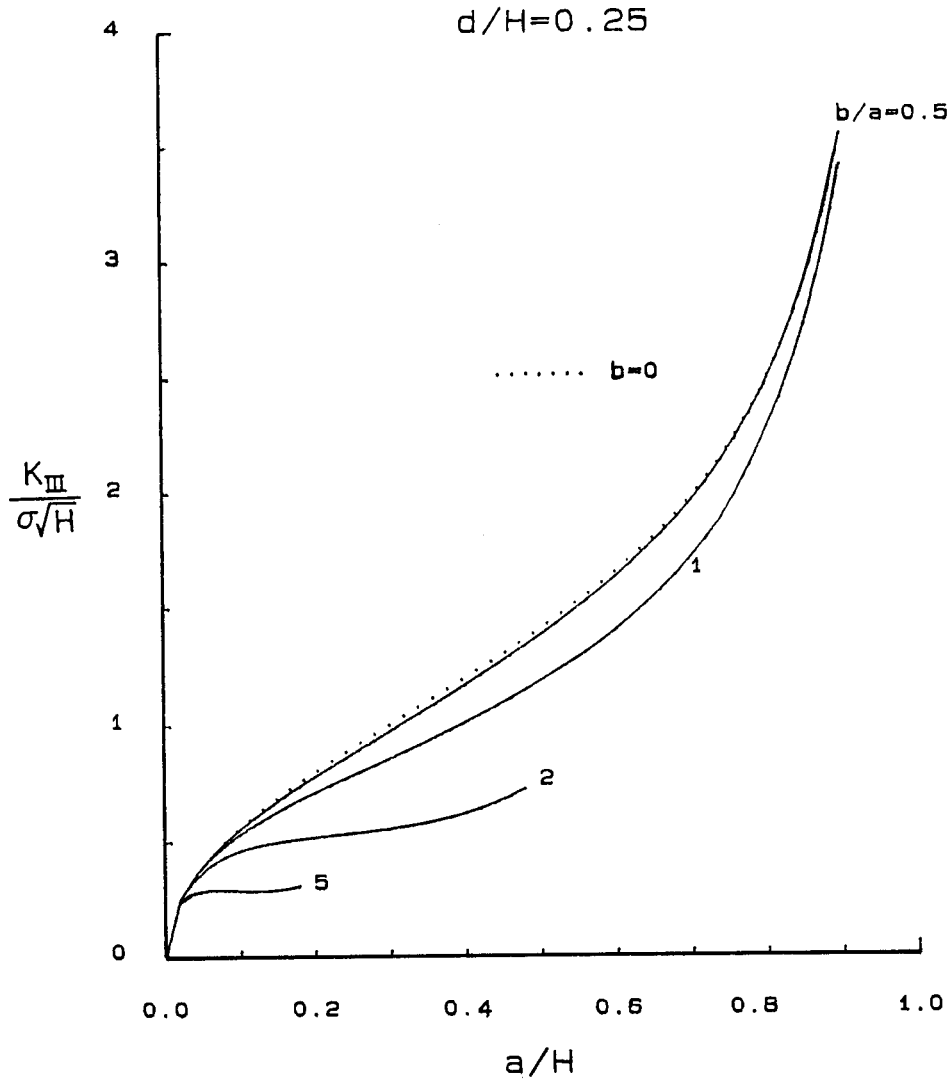

Fig. 8. Stress intensity factors at crack tip "a" for double edge cracked plate loaded by remotely applied σ.

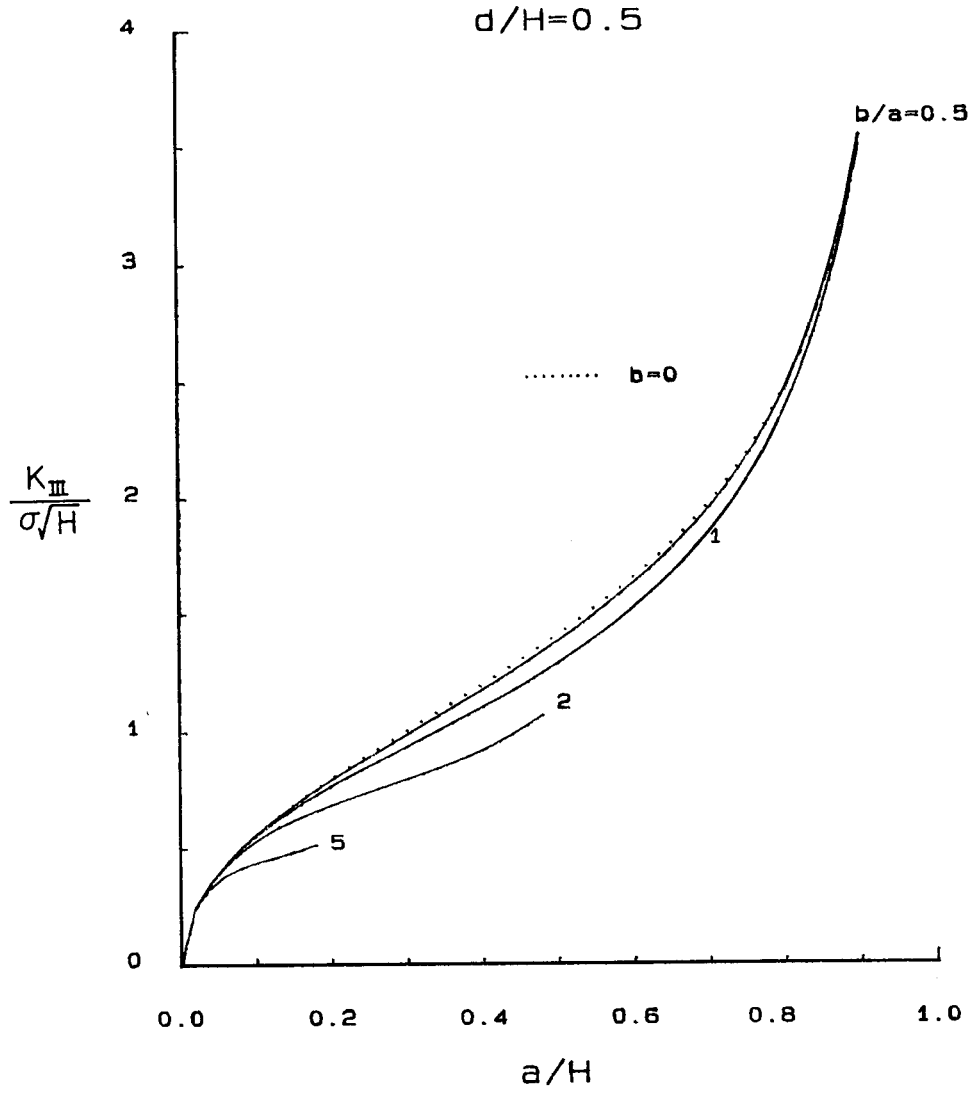

Fig. 8. Continued.

tractions at the location of crack "*a*" which are obtained by making use of the superposition method as given in (24) and using as Green's function the solution for stresses as given by (22). This alternating superposition technique is repeated until convergence of solution is obtained.

Following a similar procedure, the stress intensity factor at the crack tip due to the applied tractions can be obtained by superposition and using as Green's function equation (23), and is to be added to the stress intensity factor for the case of a single edge cracked plate loaded by a remotely applied load.

The stress intensity factors for various crack size ratios have been calculated and are shown in Fig. 8. It can be observed that the presence of a second crack "*b*" reduces the stress intensity factor at the first crack tip "*a*" for all crack size ratios. When crack "*a*" is of equal or greater size than crack "*b*", this shielding effect is greatest at intermediate crack size "*a*".

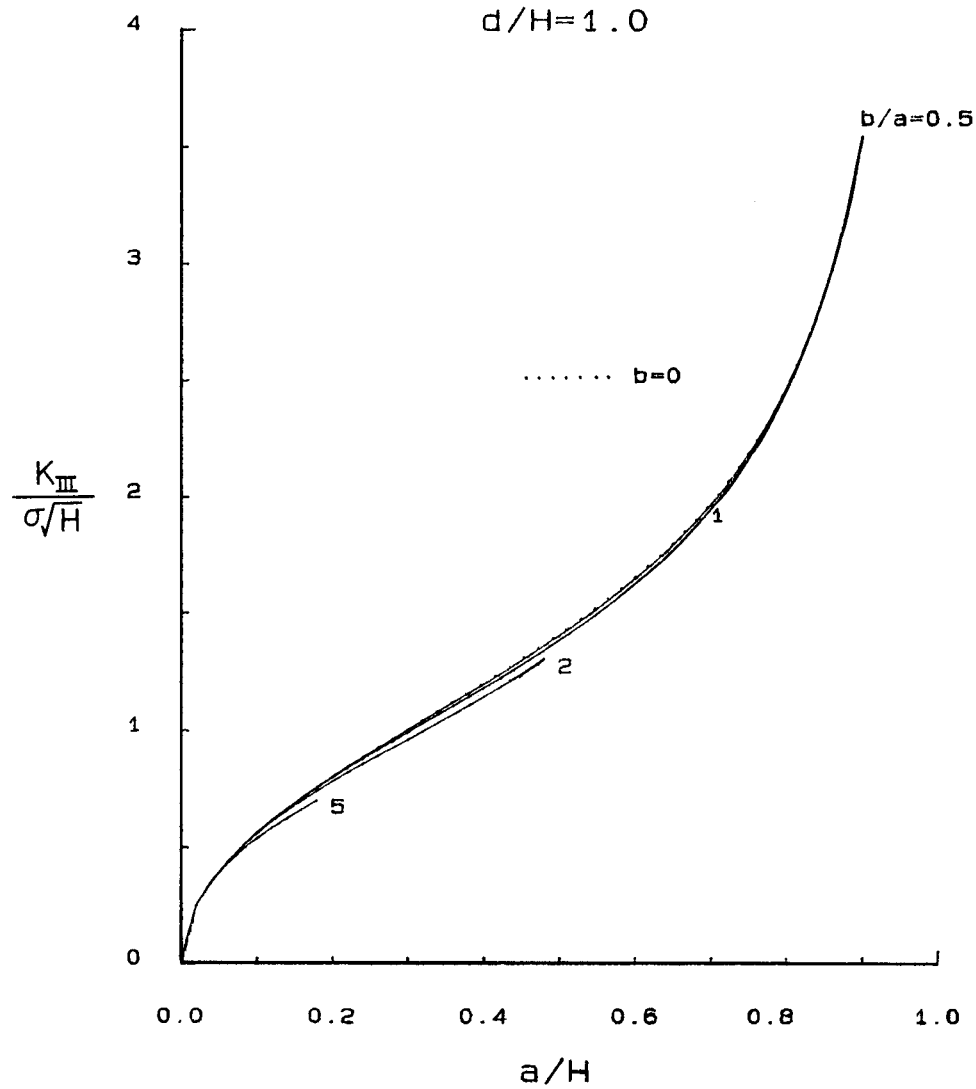

Fig. 8. Continued.

Also, at very small and very large crack size "a", the solution approaches that for a single edge cracked plate (shown as dotted line $b = 0$ in Fig. 8). As expected, the interaction between the two cracks is more pronounced the smaller the separation "d" between the two adjacent cracks. This interaction becomes negligibly small as measured against the single crack solution for any crack length ratios when $d > H$.

Acknowledgement

This work has been supported by a NASA grant to MIT. The authors would like to thank J.R. Rice for useful discussions.

References

1. H. Tada, P.C. Paris and G. Irwin, *The Stress Analysis of Cracks Handbook*, Del Research Corp., Hellertown, PA (1973).
2. P.C. Paris and G.C.M. Sih, in *Fracture Toughness Testing and Its Applications*, ASTM STP 381 (1965).
3. S. Tse, R. Dmowska and J.R. Rice, *Bulletin of the Seismological Society of America* 75, 3 (1985) 709–736.
4. V.C. Li and J.R. Rice, *Journal of Geophysical Research* 92 (1987) 11533–11551.
5. J.R. Rice, in *Fracture*, Vol. II, H. Liebowitz (ed.), Academic Press (1968).
6. H.S. Lim, "Analysis of Elastic Crack Models under Anti-plane Loadings and their Applications to the Study of Surface Deformation at Strike-slip Plate Boundaries, MIT MS thesis (1987).
7. D.L. Turcotte and D.A. Spence, *Journal of Geophysical Research* (1974) 4407–4412.

Résumé. On résoud les problèmes de dilatation antiplanaire dans une plaque élastique à fissure de bord soumise à sollicitation uniforme de surface ou à sollicitation de surface alignées, en utilisant les techniques de représentation conforme. Les solutions fornissent les distributions de contraintes, dilatations et déplacements, ainsi que les facteurs d'intensité de contraintes, dans la plaque.

Les solutions relatives aux sollicitations alignées peuvent être utilisées comme fonctions de Green pour obtenir d'autres solutions convenant pour des conditions de sollicitations de la surface plus générales. A titre d'application, on calcule le champ de déformation existant à la surface supérieure d'une plaque sousmise à des tractions arbitraires sur la surface inférieure, en recourant à une technique de superposition et aux fonctions de Green mentionnées.

En outre, on traite des facteurs d'intensité de contraintes pour deux fissures de bord dont le rapport entre les longueurs et la distance qui les sépare sont arbitraires.